Vol. 47, No. 2 (2025) 217-227, DOI: 10.24874/ti.1797.11.24.02

Tribology in Industry

www.tribology.rs

RESEARCH

Wear Behaviour of Cu-Cr-Zr Ternary Alloy for Fin-Tube Resistance Welding Electrode Material

Kiran G. Sirsath[a], Bhanudas D. Bachchhav[b,*]

[a]*Department of Technology, Savitribai Phule Pune University, Pune 411007, India,*
[b]*Department of Mechanical Engineering, All India Shri Shivaji Memorial Society's College of Engineering, Pune 411001, India.*

Keywords:

CuCrZr alloy
Wear
Full Factorial
Box Behnken
Resistance welding

* Corresponding author:

Bhanudas D. Bachchhav
E-mail: bdbachchhav@aissmscoe.com

Received: 25 November 2024
Revised: 18 January 2025
Accepted: 6 February 2025

A B S T R A C T

The wear of resistance welding electrodes negatively impacts current density and weld quality, making it essential to study their wear behavior to improve overall welding performance. This paper investigates the wear performance of a newly developed Cu-Cr-Zr alloy using a Pin-On-Disc setup, applying Full Factorial and Box-Behnken design of experiment techniques. The parameters considered were Temperature, Sliding Distance, and Force. Mathematical models for wear rate were developed using DOE method. The models were found to be statistically adequate, with p-values of 0.025 and 0.046 for the Full Factorial and Box-Behnken methods, respectively. The coefficients of determination (R^2) for these methods were 0.99 and 0.86 respectively. Statistical ANOVA analysis of the full factorial design revealed that Temperature, Sliding Distance, and Force were significant factors. However, the Box-Behnken Design indicated that only Temperature and Sliding Distance were significant factors. Contour plots and response surface plots for both DOE methods displayed an appreciable level of similarity. Further investigation into in-situ plasma-induced wear on Cu-Cr-Zr electrodes is recommended, as it could aid in designing compact fin-tube economizers.

1. INTRODUCTION

Resistance welding is widely used in industry for joining both similar and dissimilar metals, with Electrolytic Tough Pitch (ETP) copper commonly serving as the welding electrode in most applications. However, the limited lifespan of ETP copper electrodes is a significant concern, as their ductile nature leads to deformation of the electrode tip, which adversely impacts current densities, weld strength, and overall weld quality [1]. In resistance welding, heat is generated through electrical resistance at the interface of two metal surfaces. As electric current flows through these contacting surfaces under applied pressure, resistance at the interface produces heat, which fuses the metals together [2]. Electrodes typically use electrolytic tough pitch copper (ETP-Cu) for its good machinability, but its high wear rate necessitates frequent replacement, raising concerns about electrode lifespan in long-run production. Furthermore, wear of ETP copper electrodes leads to a loss of geometric form, negatively impacting product performance. Thus, a

high-performing electrode material with good wear resistance and electrical properties is essential for resistance welding. Sirsath and Bachchhav developed a ternary Copper chromium zirconium (Cu-Cr-Zr) alloy specifically for H type fin to tube welding electrode through multiple hot forging and precipitation hardening to ensure optimal electrical conductivity and high wear strength [3]. The study found that the use of the Cu-Cr-Zr alloy increased the rate of fin-to-tube resistance welding by 26%.

Wear appears as changes in material appearance and surface profile, caused by the relative motion between a component's surface and an interacting body. This progressive process accelerates with continuous operation and increased motion, leading to material detachment from the surface. Friction and wear characterization of materials is often conducted using various tribometers, with the pin-on-disc test being one of the most common. This method is popular due to its simplicity and the wide range of tribological contact conditions it can simulate [4,5].

The tribological characteristics of the base metal, as well as welding process parameters such as current, time, force, and surface roughness at the contact tip of copper alloy electrode, have been investigated by a number of researchers. Various methods have been used to select spot-welding electrode materials based on their thermal, electrical, and mechanical properties, often employing multi-attribute decision-making techniques such as AHP, preference ranking organization method for enrichment evaluation, VIKOR and WASPAS methods [6-9]. Bachchhav et al. [10] conducted a comparative investigation into the wear characteristics of Cu-Cd, Cu-Be and Cu-Cr-Zr alloys using a pin-on-disc apparatus. Under Sliding wear conditions, the Cu-Cr-Zr alloy shows promising wear resistance potential compared to both the Cu-Cd and Cu- Be alloys. Mara Leonardi et al. studied the impact of graphite granulometry on the dry Sliding behavior of copper-free friction material against pearlitic cast iron. Their findings show that both the shape and size of graphite particles affect the coefficient of friction and wear rate. Yuan Gao et al. studied the wear behavior of Cu–Sn, Cu–Ag, and Cu–Mg alloys in contact wires, finding that the friction coefficient was significantly affected by the formation of a continuous tribo-film, while plastic deformation occurred under higher loads and Sliding velocities [11].

Sharma et al. [12] investigated the friction and wear characteristics of Cu-Ti alloy under dry Sliding contacts for high-current-density pulsed-power applications, using pin-on-disc testing. Despite its excellent electrical properties, Cu-Ti showed strong anti-wear performance, making it a potential alternative to the hazardous Cu-Be alloy. Adding up to 4% titanium improved wear and corrosion resistance, but higher concentrations may cause issues.

Xing Wang et al. [13] performed a wear study using a pin-on-disc setup to analyze the effect of Zr addition in nickel-based composite coatings via cladding, which significantly refined the microstructure, enhanced wear resistance, and increased microhardness, with superior performance achieved at 4 wt.% Zr content.

Several researchers have also explored improved performance using binary copper-based alloys like Cu-Be, Cu-Ti, Cu-Cr, and Cu-Ni. Y.A. Wang et al. [14] investigated the tribological behavior of Cu-B-CrC composites, where copper serves as the main matrix and B-CrC acts as the reinforcement at concentrations of 0, 2.5, 5, and 7.5 wt.%. The tribological behavior of Cu-Be, Cu-6%Al-4%Fe, and Cu-15%Ni alloys under dry Sliding contact was examined to assess the effects of load, Sliding speed, and the formation of a tribological layer [15].

Various Design of Experiment (DOE) techniques has been employed to determine optimal levels of factors affecting wear performance of components [16]. Taguchi design experiment has displayed appreciable level of dexterity in handling optimization of various process parameters and mechanical properties. Other optimization tools such as Full Factorial Design, Genetic algorithm, artificial neural network, and Particle Swarm have been very useful over the years. Another emerging optimization tool showing high level importance is the Response Surface Methodology. Box-Behnken design is a type of Response Surface Methodology that has been known to play a great role in the optimization of process parameters. It applies the second order quadratic equation model in determining optimal values of process and response parameters. It is found to be effective in various fields of study. Its impact has been felt in engineering, medical and pharmaceutical sciences [17-19].

B. N. G. Aliemeke et al. [20] determined the optimal values of wear rate by full factorial and Box-Behnken designs successfully carried out. Also, the adjusted R^2 values of the Factorial and Box-Behnken Designs were determined to be 0.89 and 0.69 respectively. Design showed that the track diameter and the mass difference were significant with a p-value of 0.041 and 0.007 respectively. It was noticed that a reduction of wear was occasioned by an increase in track diameter and speed of the disc.

Very few studies in the open literature have analyzed the wear behavior of Cu-Cr-Zr alloys as resistance welding electrode materials. This research is significant due to its novelty in investigating the wear behavior of a Cu-Cr-Zr alloys synthesized through hot forging, intended for use as resistance welding electrodes—a material and method that have not been widely explored. The study optimizes wear parameters using statistical techniques such as Full Factorial Design and Box-Behnken Design, providing new insights into electrode performance.

2. METHODOLOGY

2.1 Materials

In this, study, a Cu-Cr-Zr ternary alloy was developed for fin-to-tube welding electrode by smelting commercial-grade plates of electrolytic copper (99.9% purity), chips of chromium, powder of zirconium, small amounts of magnesium chips and yttrium during the smelting process at 1100°C–1300°C and cast into a mould. Post-curing was done after six hours, the ingots were turned to clean the surface by removing scale. The ingot was heated again at 750°C–800°C and underwent multiple forging processes by hot pressing along its length. The alloy was subsequently precipitation hardened at a Temperature 450°C for two hour and then water quenched. Acid cleaning was done prior to machining operation and machined to get a final size. To address the potential delamination during the smelting process, the authors controlled the alloying elements, as well as the heating and cooling rates, to enhance uniformity, homogeneity, and prevent phase separation. The chemical composition for the alloy development consisted of 98.7-99.45 wt.% copper, 0.5-1.2 wt.% chromium, 0.05-0.1 wt.% zirconium, and <0.01 wt.% magnesium and yttrium. For wear testing, pins were prepared of Cu-Cr-Zr alloy with sizes 10 mm diameter and 35 mm length. The schematic and actual images of the sample pins are shown in Figure 1 a&b respectively. A small hole is drilled into one side of the pin to accommodate the Temperature sensor. The properties of Cu-Cr-Zr are presented in Table 1. Surface roughness plays a significant role in influencing the tribological performance of Sliding contacts. Surface roughness was measured using the SJ-210 Mitutoyo surface roughness device. The uniform surface finish of 0.025 μm was achieved through a precise grinding operation on all the pin samples.

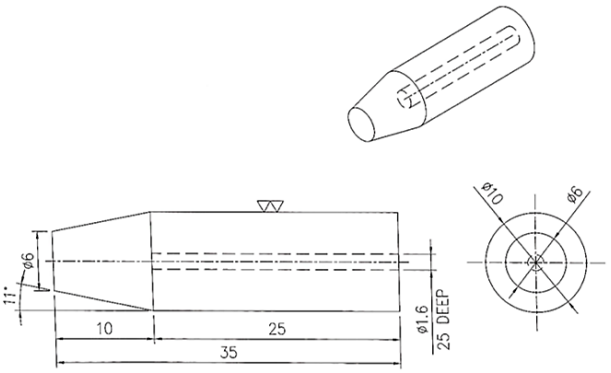

(a)

(b)

Fig. 1. (a) Schematic diagram, (b) Actual sample pins of Cu-Cr-Zr alloy.

Table 1. Properties of Cu-Cr-Zr alloy pin sample.

Parameter	Cu-Cr-Zr
Electrical Conductivity (MS/m)	49.3
Melting Point (°C)	1073
Density (Kg/m^3)	8920
Percentage Elongation (%)	18.6
Tensile Strength (MPa)	426
Hardness (HRV)	156
Thermal conductivity (@20°C W/m-K)	280

2.2 Parameter selection

Temperature, force and holding time can be simulated in Pin-on-disc apparatus, hence considered independent variables for experimentation. The experiment aims to observe the wear performance of Cu-Cr-Zr electrode materials when it subjected to various relevant conditions i.e., Temperature, Sliding Distance and Force. The temperatures of 100°C, and 300°C were chosen to represent the typical operating conditions of resistance welding electrodes, where the lower limit simulates moderate operating conditions and the upper limit simulates extreme wear scenarios. These values are based on previous studies by Bachchhav et al., and Sun et al., and practical applications, ensuring that the experimental conditions closely align with real-world scenarios [10,21,22]. These values are crucial for evaluating the wear performance under varying Temperature, which directly impacts the durability and efficiency of the electrodes. The factors and their levels for the pin-on-disc experiment are summarized in Table 2.

Table 2. Factors and their levels.

Factor	Level 1	level 2
Temperature (°C)	100	300
Sliding Distance (km)	2.35	7.06
Force (N)	50	150

2.3 Experiment test set-up

The pin-on-disc machine is depicted in the Figure 2. The device consists of a vertically oriented rotating disc made of EN-31 (AISI 52100) material and a calibrated dead-weight-loaded pin, which is held in jaws. The Pin-on-Disc setup was chosen because it effectively replicates the contact mechanism observed in resistance welding, where friction at the electrode-workpiece interface lead to electrode wear. It also considers the applied force and temperature rise at the interface, both of which impact wear. The materials, surface properties, and load conditions were tailored to replicate real-world scenarios, providing valuable insights into wear mechanisms in a controlled laboratory setting, especially when field tests are not feasible.

The stationary pin is pressed against rotating disc under the given load of 50 N and 150 N. The Sliding Distance is defined as the total distance travelled by the electrode pin while in contact with a rotating disc. Specifically, the Sliding Distance, measured in kilometres, is determined by the disc's rotational speed, the duration of rotation, and the pin's position relative to the disc's centre. In this study, the disc was rotated constantly at 500 rpm with a track radius of 50 mm for 15 minutes and 45 minutes, resulting in Sliding Distances of 2.35 km and 7.06 km, respectively.

The output response, i.e., wear (μm), was recorded from the data acquisition system. The tests were conducted as per ASTM G-99 standards. Pin-on-disc set-up was instrumented with a load cell of least 0.1N and a linear variable differential transformer (LVDT) to measure linear displacement in μm. The cylindrical pin specimen with a flat surface at one end and a hole for the Temperature sensor at the other are pressed against a rotating disc for experimentation. During the test, the friction force, wear and Temperature are continuously monitored in the Data Acquisition system (DAS) and WINDUCOM 2010 software. Each experiment was run by a separate pin sample.

The microstructure was observed under a microscope (NIKON EPIPHOT 200) by preparing an etchant of 10g FeCl3, 100 ml H2O, 50 ml HCL and 10 ml HNO3. The chemical compositions were characterized by optical emission spectra as per the BS EN 15059-2015 method. The microstructure and chemical composition of the alloy plate was characterized by scanning electron microscopy (SEM, Surpass Zeiss, Germany) coupled with energy dispersive backscatter electron spectrometry (EDS). The phase structure was examined using X-ray diffraction (XRD, D8 Advance, Bruker, Germany) with α radiation at 40 mA and 40 kV.

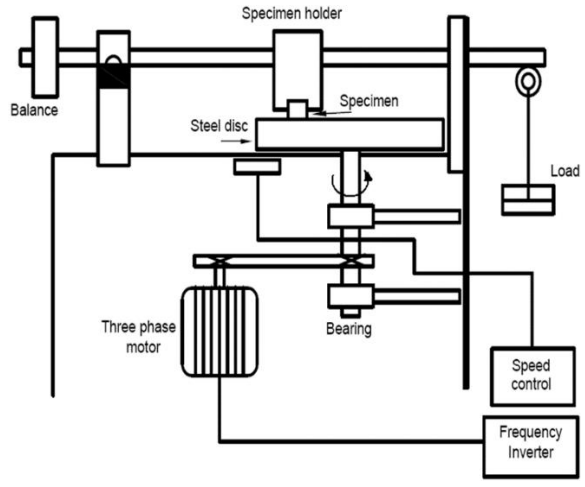

Fig. 2. Schematic of Pin-on-disc set-up.

2.4 Design of experiment

Design of experiment is a statistical approach used to identify the factors that impact the outcome of a given process. Design of experiment is a systematic, efficient method that enables the relationship between multiple input variables (factors) and key output variables (responses). It is targeted at product quality and determination of actual number of experiments to be conducted. Three types of designs are commonly used in DOE: factorial, response surface, and mixture. Each type of design is best suited for a different purpose. Factorial designs study the main effects and interactions between different independent variables. Response surface designs are used to study how a dependent variable responds to changes in one or more independent variables. Mixture designs study how two or more ingredient variables interact to produce the desired outcome. In this study the experimental layout was created for the Factorial model and the Box-Behnken Design model. The layout had columns for standard and run orders on which the experiment was conducted using the various parametric conditions as stipulated by the DOE.

The Full factorial model is the linear model applied in this study. It was applied because of its ability to economically conduct fewer numbers of experimental runs while still targeting high quality product [23]. The model contained three parameters and a range of a maximum and minimum value. This means a maximum of 8 (2^3) experiments are considered in this study, with three factors and two levels. During the experiment, a column for the response parameter was created for each experimental run. The values of the factors in Table 3 were carefully chosen to reflect the actual operating conditions experienced by resistance welding electrodes. The temperature range (100°C and 300°C) corresponds to the typical thermal conditions at the electrode interface during welding. The Sliding Distance represent realistic wear lengths encountered during repeated welding cycles. Similarly, the applied forces (50 N and 150 N) are within the range of normal forces exerted on the electrodes during operation.

The outcome of the Factorial experimentation model is shown in Table 3. The three process parameters are Temperature, Sliding Distance and Force while the response parameter is the wear rate.

Table 3. Design of experiment for the full factorial model: 2^3, 8 Runs.

Run Order	Temp. (°C)	Sliding Distance (km)	Force (N)	Wear (μm)
1	100	2.35	150	378.2
2	100	7.06	150	385.1
3	100	2.35	050	354.3
4	100	7.06	050	360.1
5	300	2.35	150	413.2
6	300	7.06	150	417.1
7	300	2.35	050	387.1
8	300	7.06	050	390.2

The Box-Behnken Design is an experimental layout of Response Surface Methodology (RSM) created to optimize process parameters and their levels. It is a nonlinear model developed to help in the estimation of responses by applying the second order quadratic response model [24]. The nonlinear model is reputed for handling minimum of 3 factors and 3 levels. Also, the Box-Behnken Design model reserves the ability of applying fewer number of runs compared to the Central Composite Design (CCD) of the Response Surface Methodology. A total number of 15 experimental runs were specified by the Minitab Software. The experiment matrix contained columns for the run orders and standard orders. The standard order which was prescribed by Minitab was used for randomizing the experiment order. The randomization effects helped in eliminating statistical selection bias and form a foundation for equality of test treatments. The Box-Behnken Design experimentation is shown in Table 4.

Table 4. Design of experiment for Box-Behnken design: 15 Run.

Run Order	Temp. (°C)	Sliding Distance (km)	Force (N)	Wear (μm)
1	300	4.705	50	418.1
2	300	7.060	100	402.2
3	200	4.705	100	384.8
4	100	4.705	50	358.7
5	200	4.705	100	384.8
6	300	2.350	100	402.1
7	200	2.350	150	370.9
8	200	2.350	50	370.8
9	200	7.060	150	399.8
10	100	7.060	100	368.3
11	200	4.705	100	384.9
12	300	4.705	150	418.4
13	100	2.350	100	368.1
14	100	4.705	150	359.0
15	200	7.060	50	399.6

3. RESULTS & DISCUSSION

The experimental and statistical analysis for the Full factorial and Box-Behnken Designs are shown in this section. Also, contained in this section are the contour and surface designs of the models considered. The wear response parameter was targeted at the smaller-the-better.

3.1 Full factorial design analysis

Table 5 gives analysis of variance results for that the parameters are significant as can be seen in Temperature, force and Sliding distance. The model is significant with a p-value 0.0000 of less than 0.05. The developed mathematical model obtained by multiple linear regression is as given in equation 1. According to the model's goodness-of-fit for Table 5, the R-squared, adjusted R-squared, predicted R-squared, and p-values are 0.9981, 0.9966, and 0.9923, and 0.025 respectively.

$$\text{Wear} = 322.79 + 0.162\ T + 1.04\ SD + 0.25F \quad (1)$$

Table 5. Analysis of variance results by the Full Factorial experiment.

Source	DF	Adj SS	Adj MS	F-Value	P-Value
Regression	3	3456.73	1152.24	694.28	0.000
Temperature	1	2107.63	2107.63	1269.95	0.000
Sliding Dist.	1	48.86	48.86	29.44	0.006
Force	1	1300.25	1300.25	783.46	0.000
Error	4	6.64	1.66		
Total	7	3463.37			

Subsequently, confirmation tests were conducted to verify the consistency of the obtained equation. Table 6 displays the experiment results, and a comparison is made between these results and the model developed in the current study (equations 1).

Table 6. Confirmation test by Full Factorial design.

Run	Temp (°C)	Sliding Dist. (km)	Force (N)	Wear (µm) Expt.	Wear (µm) Model	Error (%)
1	100	2.35	150	378.2	379.7	0.400
2	100	7.06	150	385.1	384.6	0.130
3	100	2.35	50	354.3	354.2	0.028
4	100	7.06	50	360.1	359.1	0.255
5	300	2.35	150	413.2	412.2	0.243
6	300	7.06	150	417.1	417.1	0.004
7	300	2.35	50	387.1	386.7	0.108
8	300	7.06	50	390.2	391.6	0.366

Note: Average relative error is 0.00030%

Upon analysing it is observed that the average error is anticipated to be below 1.5%, indicating the validity of the derived equation with a reasonable level of accuracy. It is evident that the predicted values and actual values obtained from the FFD of experiment are very close which shows that the distribution is normal. Also, there is no noticeable outlier in the distribution also confirms that the predicted and actual values were very close. The contour plot shown in Figure 3, depicts that rate of wear was significant majorly due to Temperature and force.

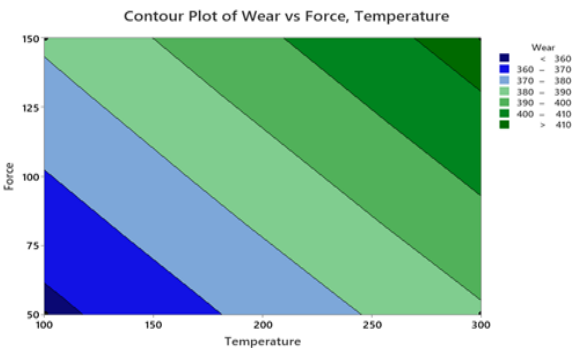

Fig. 3. Contour plot wear vs force & temperature by full factorial design.

3.2 Box-Behnken Design Analysis

The Design of Experiment platform applied in the Box-Behnken response surface methodology is shown in Table 4. A total number of 15 experimental runs conducted. Table 7 gives analysis of variance results for that the parameters are significant as can be seen in Temperature, and Sliding distance. According to the model's goodness-of-fit for Table 7, the R-squared, adjusted R-squared, predicted R-squared and p-values are 0.8615, 0.8338, 0.7042, and 0.046 respectively. The model is significant with a p-value 0.0000 of less than 0.05. Additionally, parameters such as force were observed to be insignificant due to their p-value of 0.974, which is greater than 0.05, and thus can be discarded from the regression model. The developed mathematical model obtained by multiple linear regression is as given in equation 2. The inclusion of force does not introduce any significant multicollinearity or adversely affect the model's fit within the selected rage. The R^2 value of 0.8615 suggests a strong model with the included predictors. The statistical significance is not supported in this case, its inclusion may still be useful for completeness in understanding the relationship between all potential factors.

$$\text{Wear} = 324.673 + 0.233\ T + 3.086\ SD \quad (2)$$

Table 7. Analysis of Variance results by the Box-Behnken Design

Source	DF	Adj SS	Adj MS	F-Value	P-Value
Regression	3	4781.77	1593.92	22.81	0.000
Temperature	1	4359.45	4359.45	62.39	0.000
Sliding Dist.	1	422.24	422.24	6.04	0.032
Force	1	0.08	0.08	0.00	0.974
Error	11	768.58	69.87		
Lack-of-Fit	9	768.58	85.40	69241.3	0.000
Pure Error	2	0.00	0.00		
Total	14	5550.35			

Although the Box-Behnken Design does not demonstrate the statistical significance of Force within the selected range, its inclusion enhances modeling flexibility and may provide valuable insights when considering a broader parameter range or different in-situ experimental conditions.

Table 8. Confirmation test by Box-Behnken Design

RUN	Temp (°C)	Slid. Dist. (km)	Force (N)	Wear (μm) Exp.	Wear (μm) Model	Error (%)
1	300	4.705	50	418.1	411.8	1.53
2	300	7.06	100	402.2	415.8	-3.25
3	200	4.705	100	384.8	384.8	0.00
4	100	4.705	50	358.7	365.1	-1.75
5	200	4.705	100	384.8	384.8	-0.01
6	300	2.35	100	402.1	401.3	0.20
7	200	2.35	150	370.9	378.1	-1.91
8	200	2.35	50	370.8	378.0	-1.89
9	200	7.06	150	399.8	392.7	1.82
10	100	7.06	100	368.3	369.1	-0.22
11	200	4.705	100	384.9	384.8	0.01
12	300	4.705	150	418.4	412.0	1.55
13	100	2.35	100	368.1	354.5	3.81
14	100	4.705	150	359.0	365.3	-1.73
15	200	7.06	50	399.6	392.4	1.84

Note: Average relative error is 0.00060%

Subsequently, confirmation tests were conducted to verify the consistency of the obtained equation. Table 8 displays the experiment results, and a comparison is made between these results and the model developed in the current study equations 3 using experimentally obtained values. It is observed that the average error is anticipated to be below 1.5%, indicating the validity of the derived equation with a reasonable level of accuracy.

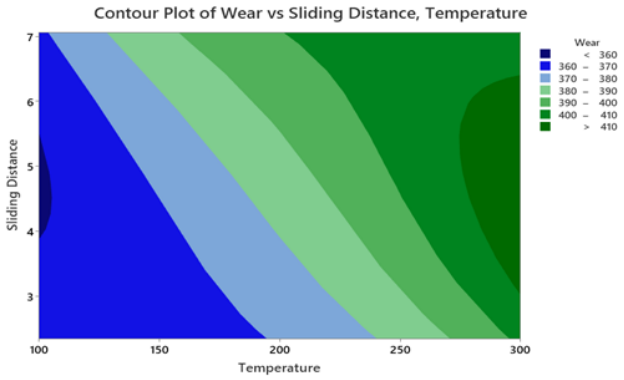

Fig. 4. Contour plot wear vs sliding distance & temperature by Box-Behnken design.

The contour plot shown in Figure 4, depicts that rate of wear was significant majorly due to Temperature and Sliding distance. The response surface plots shown in Figures 5, clearly indicates the magnitude and regions where wear rate occurs when Temperature and Sliding distance parameters increase of 200 °C and 4.7 km at 100 N force.

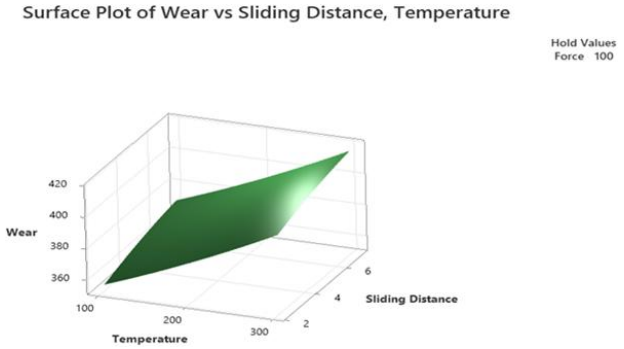

Fig. 5. Contour Plot Wear vs Sliding Distance & Temperature by Box-Behnken Design.

3.3 Morphologies analysis

Figure 6 shows morphologies of Cu-Cr-Zr alloy of test run of optimum at 200°C Temperature, Sliding distance of 4.7 km and 100 N force. The worn surface of the pin samples was examined using SEM at 500x magnification level. Small wear debris with light furrows were observed on the worn surface of Cu-Cr-Zr. Both adhesive and abrasive wear mechanisms were observed due to ploughing and presence of wear particles. The results obtained by Bachchhav et al. and Purcek et al. reinforce the present findings, indicating that the creation of tribo-layers at elevated Temperatures significantly influences the wear experienced in copper-induced metallized carbon materials [10,19,21].

This indicates metal transfer and adhesive type of wear due to high shear and low everyday stresses. Abrasive wear with light furrows was observed on the worn surface at 100N force due to hard asperities present on the EN31 disc surface and repeated Sliding Hence, both adhesive and abrasive wear mechanism was observed. An amount of wear is correlated to a rise in Temperature and contact pressure on Sliding interfaces; similar results were reported by researchers [25-26]. An increase in Temperature may cause localised welding, which leads to severe plastic deformation/ploughing under Sliding conditions. Thermal degradation of the ingredients is also involved in controlling the amount of wear in the case of friction materials. Black oxide-like layers form on the Cu-Cr-Zr surface, helping to minimize wear. Chromium typically enhances the hardness and wear resistance of copper alloys. When the chromium content increases, it forms hard carbide phases like [27] (Cr, W)7C3 and (Cr, W)3C2, which can significantly improve the wear resistance. These carbide phases help resist wear by providing a harder phase within the matrix, which reduces material loss during Sliding contact. At higher chromium concentrations, the alloy may develop a more refined microstructure with stronger intermetallic bonds, improving the alloy's ability to withstand frictional forces. The presence of Zr can alter the frictional behaviour of the alloy, making it more stable under varying wear conditions. Zr-rich alloys tend to perform better under high-load or high-temperature conditions [28] due to their ability to form stable oxide layers that protect the underlying material from further degradation. This result shows that the developed Cu-Cr-Zr alloy more like exhibits superior wear resistance. Hence, Cu-Cr-Zr can be the best alternative material for the resistance welding electrode [29-30].

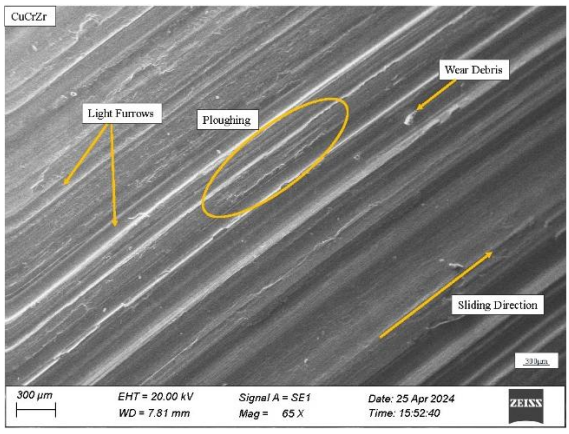

Fig. 6. Morphologies of CuCrZr alloy under optimum condition 200°C, 4.7 km, 100N.

The worn surface of the pin samples was examined using a scanning electron microscope at 100x magnification. Figure 7 shows the SEM & EDS results for optimum run at 200°C Temperature, Sliding distance of 4.7 km and 100 N force. The chemical composition was found to be homogeneous and matched that of the base material. No additional impurities were detected on the analyzed worn surface, indicating good wear strength of CuCrZr alloy.

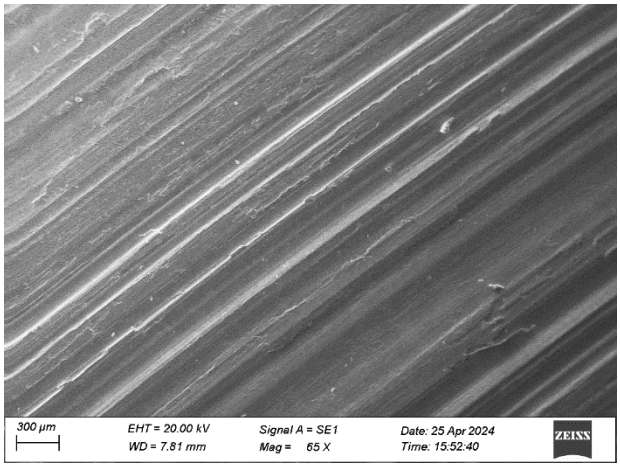

(a)

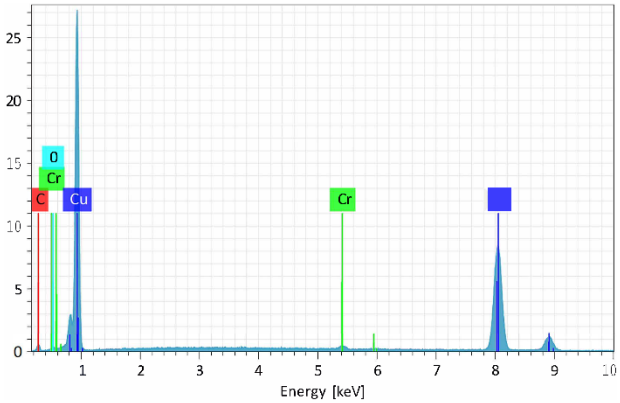

(b)

Fig. 7. (a) SEM Image, (b) EDS image of worn surface of Cu-Cr-Zr alloy for 200°C, 4.7 km and 100N.

Figure 8 shows the microstructure of the pin sample, which was observed under a microscope. The effective grain size of the alloy was measured to be 267 nm. The micron-sized precipitated Cr phase adopts a body-centered cubic (BCC) structure, as documented in the literature [31]. Notably, Cr phases precipitated from the Copper substrate, leading to significant relief of lattice distortion compared to the solid solution state. Additionally, some misfit dislocations were observed in the substrate. The grain boundary, with its high density of dislocations and some precipitation strengthening, contributes to the increase in yield strength of the developed alloy. Furthermore, the copper chromium zirconium alloy electrode can be selected to demonstrate great strength for H-type resistance fin to tube welding application.

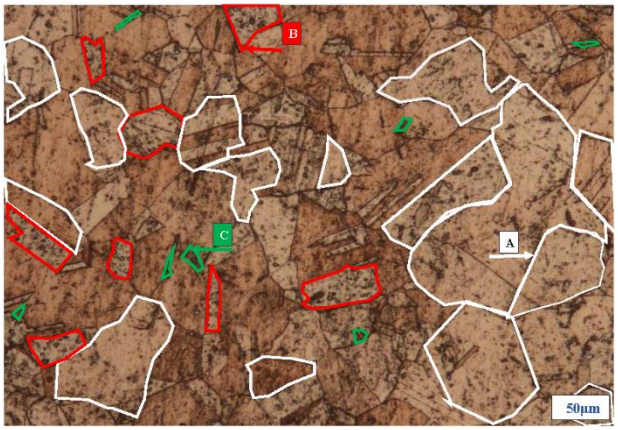

Fig. 8. Microstructure of Cu-Cr-Zr alloy of worn surface A) Grain boundary with high density dislocation B) Diffuse distribution of precipitates C) Micron precipitates.

This unique synthesis of the Cu-Cr-Zr alloy through hot forging improves material properties, making it ideal for high-performance welding applications. The findings not only enhance understanding of electrode wear but also provide practical solutions to improve welding quality, electrode lifespan, and process efficiency. This research contributes to both the welding industry and other applications, such as compact heat exchangers, promoting more sustainable and efficient industrial processes

4. CONCLUSION

Full Factorial and Box-Behnken design methods were successfully applied on the wear response of a copper chromium zirconium ternary alloy using pin-on-disc parameters such as Temperature, Sliding Distance and Force. The data fitting analysis carried out on the first order and quadratic models showed that latter had the best fit and better adjusted R^2 values which qualified it to be used to navigate through the design space in order to obtain optimal values.

1. The developed mathematical model for the factorial and Box-Behnken Design methods were found to be adequate with a p-value of 0.025 and 0.046 respectively.

2. The adjusted R^2 values of Factorial and Box-Behnken Design were 0.99 and 0.86 respectively. This served as pointers that the developed mathematical models are significant.
3. The factorial method and the Box-Behnken Design showed some similarities in the contour plots and response surface plots. Some of the similarities were found in the reduction of wear rate which was occasioned by the Temperature and Force. Also, an increase in Sliding Distance resulted in moderate increase in wear rate.
4. Chromium primarily enhances hardness and wear resistance by forming carbide phases, while zirconium improves the alloy's strength and wear resistance at high temperatures through fine precipitates and grain refinement. The wear performance also depends on the balance of these elements, their distribution within the matrix, and the structural state after forging, including the effects of heat treatment.

Further investigation on the measurement of in-situ wear due to plasma and its impact on the metallurgical characteristics of Cu-Cr-Zr electrode is recommended

REFERENCES

[1] H. Chen, Y. Wang, Q. Zhao, H. Ma, Y. Li, and Z. Chen, "Experimental investigation of heat transfer and pressure drop characteristics of H-type finned tube banks," *Energies*, vol. 7, no. 11, pp. 7094–7104, Nov. 2014, doi: 10.3390/en7117094.

[2] K. Zhou and P. Yao, "Overview of recent advances of process analysis and quality control in resistance spot welding," *Mechanical Systems and Signal Processing*, vol. 124, pp. 170–198, Feb. 2019, doi: 10.1016/j.ymssp.2019.01.041.

[3] H. Chen, Y. Wang, Q. Zhao, H. Ma, Y. Li, and Z. Chen, "Experimental investigation of heat transfer and pressure drop characteristics of H-type finned tube banks," *Energies*, vol. 7, no. 11, pp. 7094–7104, Nov. 2014, doi: 10.3390/en7117094.

[4] K. G. Sirsath and B. D. Bachchhav, "Tribo-mechanical characterization of Cu-Cr-Zr ternary alloy aimed at fin-tube resistance welding electrode material," *Industrial Lubrication and Tribology*, vol. 75, no. 8, pp. 942–949, Aug. 2023, doi: 10.1108/ilt-04-2023-0092.

[5] "Pin-on-Disk Wear Testing," *Element*. https://www.element.com/life-sciences/medical-device/pin-on-disk-wear-testing.

[6] Y. Lyu, E. Bergseth, and U. Olofsson, "Open system tribology and influence of weather condition," *Scientific Reports*, vol. 6, no. 1, Aug. 2016, doi: 10.1038/srep32455.

[7] B. Bachchhav, S. Bharne, A. Choudhari, and S. Pattanshetti, "Selection of spot welding electrode material by AHP, TOPSIS, and SAW," *Materials Today Proceedings*, Mar. 2023, doi: 10.1016/j.matpr.2023.02.253.

[8] Bachchhav, A. Kumbhare, C. Hoonur, S. Kulkarni, and J. Kalankar, "Grading of spot welding electrode material properties using AHP," *Journal of Modern Mechanical Engineering and Technology*, vol. 7, pp. 59–65, Jun. 2020, doi: 10.31875/2409-9848.2020.07.8.

[9] M. Leonardi, M. Alemani, G. Straffelini, and S. Gialanella, "A pin-on-disc study on the dry sliding behavior of a Cu-free friction material containing different types of natural graphite," *Wear*, vol. 442–443, p. 203157, Dec. 2019, doi: 10.1016/j.wear.2019.203157.

[10] B. D. Bachchhav, S. V. Chaitanya, S. Salunkhe, P. Chandrakumar, M. Pagáč, and E. A. Nasr, "Wear performance of CU–CD, CU–BE and CU–CR–ZR spot welding electrode materials," *Lubricants*, vol. 11, no. 7, p. 291, Jul. 2023, doi: 10.3390/lubricants11070291.

[11] Y. Gao, J.-C. Jie, P.-C. Zhang, J. Zhang, T.-M. Wang, and T.-J. Li, "Wear behavior of high strength and high conductivity Cu alloys under dry sliding," *Transactions of Nonferrous Metals Society of China*, vol. 25, no. 7, pp. 2293–2300, Jul. 2015, doi: 10.1016/s1003-6326(15)63844-4.

[12] M. D. Sharma and R. Sehgal, "Dry sliding friction and wear behaviour of titanium alloy (TI-6AL-4V)," *Tribology Online*, vol. 7, no. 2, pp. 87–95, Jan. 2012, doi: 10.2474/trol.7.87.

[13] X. Wang *et al.*, "Investigation on the effects of Zr alloying on in-situ synthesis of dual-scale reinforcement and wear resistance of wide-band laser clad nickel composite coatings," *Optics & Laser Technology*, vol. 183, p. 112240, Dec. 2024, doi: 10.1016/j.optlastec.2024.112240.

[14] Y. A. Wang, J. X. Li, Y. Yan, and L. J. Qiao, "Effect of electrical current on tribological behavior of copper-impregnated metallized carbon against a Cu–Cr–Zr alloy," *Tribology International*, vol. 50, pp. 26–34, Jan. 2012, doi: 10.1016/j.triboint.2011.12.022.

[15] G. Straffelini, L. Maines, M. Pellizzari, and P. Scardi, "Dry sliding wear of Cu–Be alloys," *Wear*,

vol. 259, no. 1–6, pp. 506–511, Jan. 2005, doi: 10.1016/j.wear.2004.11.013.

[16] A. P. Zhilyaev, A. Morozova, J. M. Cabrera, R. Kaibyshev, and T. G. Langdon, "Wear resistance and electroconductivity in a Cu–0.3Cr–0.5Zr alloy processed by ECAP," *Journal of Materials Science*, vol. 52, no. 1, pp. 305–313, Aug. 2016, doi: 10.1007/s10853-016-0331-8.

[17] D. V. Shangina, N. R. Bochvar, A. I. Morozova, A. N. Belyakov, R. O. Kaibyshev, and S. V. Dobatkin, "Effect of chromium and zirconium content on structure, strength and electrical conductivity of Cu-Cr-Zr alloys after high pressure torsion," *Materials Letters*, vol. 199, pp. 46–49, Apr. 2017, doi: 10.1016/j.matlet.2017.04.039.

[18] M. A. Shaik and B. R. Golla, "Development of highly wear resistant Cu - Al alloys processed via powder metallurgy," *Tribology International*, vol. 136, pp. 127–139, Mar. 2019, doi: 10.1016/j.triboint.2019.03.055.

[19] G. Purcek, H. Yanar, O. Saray, I. Karaman, and H. J. Maier, "Effect of precipitation on mechanical and wear properties of ultrafine-grained Cu–Cr–Zr alloy," *Wear*, vol. 311, no. 1–2, pp. 149–158, Jan. 2014, doi: 10.1016/j.wear.2014.01.007.

[20] B. N. G. Aliemeke, H. A. Okwudibe, A. I. Omoakhalen, and P. Major, "Box-Behnken optimization of pin-on-disc wear test process parameters," *Nigerian Journal of Technology*, vol. 42, no. 4, pp. 464–471, Feb. 2024, doi: 10.4314/njt.v42i4.6.

[21] B. D. Bachchhav and H. Bagchi, "Tribological Performance of Copper-Titanium Alloy under Dry Sliding Contact," *Materials Performance and Characterization*, vol. 10, no. 1, pp. 739–750, Nov. 2021, doi: 10.1520/mpc20200177.

[22] H. T. Sun, X. M. Lai, Y. S. Zhang, and J. Shen, "Effect of variable electrode force on weld quality in resistance spot welding," *Science and Technology of Welding & Joining*, vol. 12, no. 8, pp. 718–724, Nov. 2007, doi: 10.1179/174329307x251862.

[23] G. Purcek, H. Yanar, M. Demirtas, D. V. Shangina, N. R. Bochvar, and S. V. Dobatkin, "Microstructural, mechanical and tribological properties of ultrafine-grained Cu–Cr–Zr alloy processed by high pressure torsion," *Journal of Alloys and Compounds*, vol. 816, p. 152675, Oct. 2019, doi: 10.1016/j.jallcom.2019.152675.

[24] Ü. A. Usca, M. Uzun, M. Kuntoğlu, S. Şap, K. Giasin, and D. Y. Pimenov, "Tribological aspects, optimization and analysis of CU-B-CRC composites fabricated by powder metallurgy," *Materials*, vol. 14, no. 15, p. 4217, Jul. 2021, doi: 10.3390/ma14154217.

[25] W. Wei, F. Sun, Y. Shi, L. Ma, and J. Liu, "Experimental Study of Heat Transfer and Resistance Characteristics of Single H-Type and Double H-Type Finned Tubes," *POWER ICOPE*, Jun. 2017, doi: 10.1115/power-icope2017-3289.

[26] K. Zhou and P. Yao, "Overview of recent advances of process analysis and quality control in resistance spot welding," *Mechanical Systems and Signal Processing*, vol. 124, pp. 170–198, Feb. 2019, doi: 10.1016/j.ymssp.2019.01.041.

[27] Z. Li *et al.*, "Effects of different Cr contents on microstructure, mechanical and electrical properties of Cu-Zr-Cr alloy," *Materials Today Communications*, vol. 38, p. 108408, Feb. 2024, doi: 10.1016/j.mtcomm.2024.108408.

[28] J. Park, M. Ahn, G. Yu, J. Kim, S. Kim, C. Shin, "Influence of alloying elements and composition on microstructure and mechanical properties of Cu-Si, Cu-Ag, Cu-Ti, and Cu-Zr alloys," *Materials Today Communications*, vol. 38, p. 107821, 2024, doi: 10.1016/j.mtcomm.2023.10782.

[29] Z. Wan, H.-P. Wang, M. Wang, B. E. Carlson, and D. R. Sigler, "Numerical simulation of resistance spot welding of Al to zinc-coated steel with improved representation of contact interactions," *International Journal of Heat and Mass Transfer*, vol. 101, pp. 749–763, Jun. 2016, doi: 10.1016/j.ijheatmasstransfer.2016.05.023.

[30] M. Sheikhi, M. Valaee-Tale, Y. Mazaheri, and G. R. Usefifar, "Electrode lifetime in resistance spot welding of coated sheets: Experiments and modeling," *Materials Today Communications*, vol. 38, p. 107903, Dec. 2023, doi: 10.1016/j.mtcomm.2023.107903.

[31] J. Li, H. Ding, B. Li, and L. Wang, "Microstructure evolution and properties of a Cu–Cr–Zr alloy with high strength and high conductivity," *Materials Science and Engineering A*, vol. 819, p. 141464, May 2021, doi: 10.1016/j.msea.2021.141464.